

Elemental nanoimaging of monazite and zircon using a confocal detection scheme

K. Appel, P. Appel¹ and A. Möller²

HASYLAB at DESY, Notkestrasse 85, 22603 Hamburg, Germany

¹Institute of Geosciences, CAU Kiel, Ludwig-Meyn Straße 10, 24098 Kiel, Germany

²Department of Geology, University of Kansas, Lawrence, KS, U.S.A.

A wealth of geoscientific information on rock formation can be derived from trace elements such as rare earth elements (REE) or U, Th, Pb in accessory minerals (see also [1]). While REE patterns are widely used to study conditions present during continental crust formation, U, Th and Pb concentrations are used for age dating of metamorphic and igneous processes. So far, age dating and trace element detection have been performed with different methods. In this study, we apply for the first time, combined elemental imaging with chemical age dating at sub-micrometer resolution using XRF mapping. The study was performed on the accessory minerals monazite (LREE, Ca,Th,U)PO₄ and zircon (ZrSiO₄) which incorporate U and Th during formation, are stable over a wide P-T (pressure-temperature) range up to ultra-high temperature conditions (T >900°C) and widespread in different bulk rock compositions.

Measurements were performed at the nanoimaging beamline ID22NI at ESRF, Grenoble. The excitation energy was set to 17.6 keV in order to allow the simultaneous detection of REE and Pb, Th and U via L-shell excitation and elements with Z between 14 and 39 via K-shell excitation, but exclude the excitation of the Zr K-edge. A 1.5 mm Al absorber was introduced to reduce the background in the low energy region. The incoming beam was focused with the KB-mirror system to spot size of 190 nm horizontally and 164 nm vertically. This configuration resulted in a photon flux on the sample of 5×10^9 ph/sec. Fluorescence signals were recorded with an energy-dispersive SDD detector in confocal geometry using a polycapillary half-lens on the detection side (Figure 1). The confocal geometry resulted in a detector acceptance of less than 15 μm in the energy range with the emission lines of interest for chemical age dating (Pb-L α , Th-L3M1 and U-L3M1; Figure 2). Six known age reference samples for monazite were measured in order to establish a method for chemical age dating of monazite. No method exists so far for zircon and is objective of this study. 2D elemental maps were always performed in the layer of the sample yielding maximum fluorescence signal. Sample times varied between 0.4 and 50 sec and maximum step sizes were 0.25 μm. Peak areas were fitted using PyMCA [2].

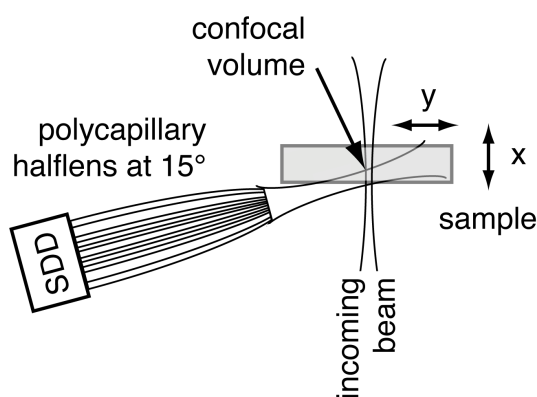


Figure 1: Confocal geometry at ID22NI.

detector acceptance based on foil scans

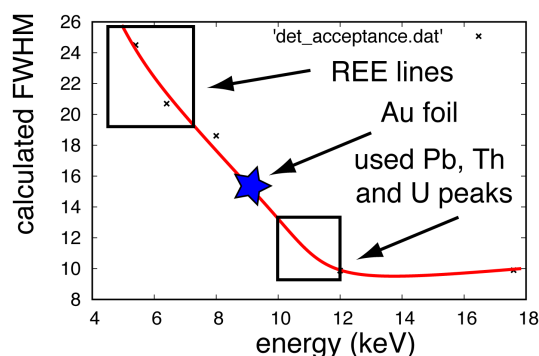


Figure 2: Characterisation of the confocal set-up: the results are based on measurements of foils.

Chemical age dating at the nano-scale:[3] showed that chemical ages using confocal micro-fluorescence can be calculated from fluorescence intensities of Pb, Th and U using the Ranchin formula:

$$Age_{ref} = \frac{k_{Pb} \cdot I_{Pb}}{k_U \cdot I_U + 0.36 \cdot k_{Th} \cdot I_{Th}}$$

The parameters k_x can be retrieved iteratively by measurements of a reference sample. In this study, we used six reference monazite samples with an age range between 101 Ma and 1821 Ma (Figure 3). With this method, an precision of 10 % could be found, however, measured ages still differ by up to 7 % to the reference ages. In the next step it will be tested, whether accuracy can be improved by calculation of the ages using concentrations of Pb, Th and U instead of peak areas.

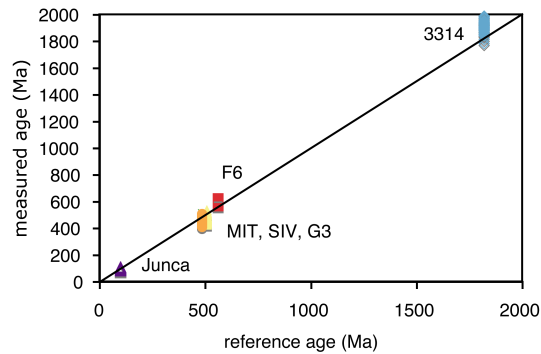


Figure 3: Determined ages for age reference samples vs. reference ages in Ma.

Elemental nanoimaging reveals different effects: while the example displayed in Figure 4a shows that the boundary between the inherited core in zircon and the overgrowth was sharp on 250 nm scale, indicating this to be a true overgrowth with minimal or no recrystallisation and scavenging of the core, the examples on the right (Figure 4b) document polymetamorphic growth with diffuse boundaries (top) and later changes due to hydrothermal activity (bottom) in monazite (Figure 4c).

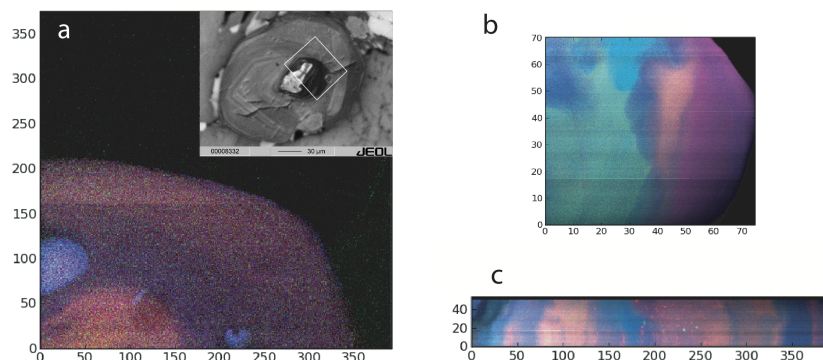


Figure 4: U (red)-Pb(green)-Th(blue) tri color maps of monazite and zircon from three crustal environments.

References

- [1] K. Appel, P. Appel, HASYLAB annual report (2009), 2009613.pdf.
- [2] V.A. Sole, E. Papillon, M. Cotte, Ph. Walter, J. Susini, Spectrochim. Acta B 62, 63 (2007).
- [3] S. Schmitz, A. Möller, M. Wilke, W. Malzer, B. Kanngiesser, R. Bousquet, A. Berger, S. Schefer Eur. J. Mineral. 21, 927 (2009).